CONTROL AUGMENTED STRUCTURAL SYNTHESIS WITH TRANSIENT RESPONSE CONSTRAINTS*

R. A. Manning**

and

L. A. Schmit***

University of California, Los Angeles

Los Angeles, California

AIAA Paper No. 87-0749-CP

to be presented at the

AIAA/ASME/ASCE/AHS

28th Structures, Structural Dynamics, and Materials Conference

Monterey, California

April 6-8, 1987

*This research was carried out under NASA Research Grant No. NSG-1490 with supplementary support from GM Research Laboratories.

** Graduate Research Assistant,

Student Member AIAA, Student Member ASME

*** Professor of Engineering and Applied Science,

Fellow ASCE, Fellow AIAA

Abstract

An integrated approach to the optimum design of control augmented structural systems is presented in which structural variables and control variables are changed simultaneously during the design process. Constraints are imposed on peak transient dynamic displacements and accelerations, static displacements, natural frequencies, and control system effort. Side constraints imposed on structural member sizes and control system thresholds and actuator output forces insure the generation of physically meaningful designs. Example problems are presented which bring out the benefits of simultaneous treatment of both the structural design variables and the control design variables.

Introduction

Interest in large flexible space structures has stimulated research efforts aimed at integrating the design of structural and control systems. In many instances the goal of this integrated design task is to minimize the total system mass while satisfying deformation criteria and control system limitations.

In the past, the usual technique for designing these systems has been to fix either the structural or control system design, and redesign the other to improve the fixed system's performance characteristics [1 – 3] . However, recent investigations [4 – 6] have shown the synergistic nature of active and passive design techniques.

As a result, a number of simultaneous design methods have been suggested in the literature.

These simultaneous structural/control approaches, however, are sequential in nature within an iterative framework. For example, Messac and Turner [7] relate the optimal controls to the structural design variables and then formulate the design problem in terms of structural variables alone.

A more unified approach to the structural/control design problem has been presented by Bodden, Junkins et. al. [8 – 9]. Their design optimization strategies change both structural (passive) variables and control (active) variables to improve system performance. In Ref. 8, a minimum modification strategy is developed which uses either direct output feedback control or steady state regulator control in conjunction with two distinct objective functions, namely, eigenvalue placement and minimum control gain Euclidian norm [8, Eq. 62]. In Ref. 9, an eigenspace optimization approach is presented in which structural parameters, sensor/actuator locations, and control feedback gains are included in the set of variables that may be changed during the design process.

Previously reported studies, with the exception of Ref. 10, do not include direct consideration of dynamic response constraints, actuator force constraints, and static response constraints. The control augmented structural synthesis work reported in Ref. 10 was limited to linear feedback control systems and it was assumed that the dynamic loading conditions were harmonic, so that steady state dynamic response

was of primary interest. The research results reported here will consider transient dynamic response to arbitrary forcing functions as well as the use of nonlinear on/off controllers.

In this paper, an integrated approach to control augmented structural synthesis is presented in which both the structural (passive) variables and the control (active) variables may be changed in order to obtain minimum objective function designs. Constraints on system performance include transient dynamic displacement and/or acceleration constraints, control actuator force upper bounds, control system effort constraints, and a structural mass upper bound. Either structural mass or control effort may be chosen as the objective function to be minimized. The optimum design is found by solving a sequence of approximate problems using a wide range of approximation concepts.

Optimum Design Problem Statement

The design problem posed in the introduction may be stated as: Find the vector of design variables, d, such that some composite objective function, $W+E$, is a minimum and the behavior constraints, g_m, are satisfied. Mathematically, this can be written as: Find the vector d such that

$$\min \left[W(d) + \int_0^{t_f} E(d,t)dt \right] \tag{1}$$

subject to

$$g_m(d,t) \geq 0 \tag{2}$$

and

$$d^l \leq d \leq d^u \tag{3}$$

where W is the total weight of the structure plus nonstructural masses and E is the control system effort.

The vector of design variables, d, is made up of beam design element section properties, nonstructural mass design element radii, control actuator thresholds and output forces. The structure is assumed to have fixed configuration, topology, and material.

The twelve degree-of-freedom box beam finite elements shown in Figure 1 are used to model the structures. A number of analysis elements may be linked to a single design element and, additionally, linking within the cross-section of the design element is allowed. Direct section properties are used as the structural variables in the optimization.

Nonstructural masses can either be fixed for model definition or be varied during the optimum design process. The nonstructural masses (see Figure 2) consist of spherical elements of specified material and either fixed radii or variable radii (depending on whether the nonstructural masses are used as design elements).

The control system consists of a given number of sensors at specified degrees-of-freedom and a fixed number of control actuators or thrusters at specified degrees-of-freedom. The characteristics of the sensors are invariant during the design process and allow a set of output measurements, Y_n and $\dot{Y}_n$, to be obtained. Based on these output

measurements, the actuators produce control forces in an attempt to reduce dynamic response.

Two different control laws have been used. The first (referred to as Type I, see Appendix A) uses both displacement and velocity measurements to determine the output control forces and the second (Type II) uses velocity measurements only. For example, the Type II control law utilizes velocity measurements, $\dot{Y}_n$, to produce output forces, u_n, according to the relations

$$u_n = \begin{cases} 0 \text{ if } |\dot{Y}_n| \le \varepsilon_n \\ -\bar{u}_n \text{ if } |\dot{Y}_n| \ge \varepsilon_n \text{ and } \dot{Y}_n \ge 0 \\ +\bar{u}_n \text{ if } |\dot{Y}_n| \ge \varepsilon_n \text{ and } \dot{Y}_n \le 0 \\ 0 \text{ otherwise} \end{cases} \tag{4}$$

where the velocity threshold, ε_n, and the output force, $\bar{u}_n$, are used as the design variables. A small amount of vibration is tolerable as indicated by the presence of the velocity threshold, but any vibration past this level activates the control system.

The set of constraints, g_m, contains static displacement and/or rotation constraints, dynamic displacement and/or rotation constraints, dynamic translational and/or rotational acceleration constraints, and natural frequency constraints. It should be noted that all of the behavior constraints represented by g_m are time parametric in nature except for the static constraints and the natural frequency constraints.

The side constraints in equation (3) represent upper and lower bounds on the beam element cross sectional dimensions which have been transformed to section property side constraints, as well as upper and

lower bounds on the nonstructural mass and control system design variables. The side constraints are necessary to satisfy analysis validity limitations in addition to other designer-specified guidelines.

In general, the optimum design problem represented by equations (1) through (3) is a complex, nonlinear mathematical programming problem which precludes direct solution attempts even in the absence of time parametric constraints [11].

The composite objective function design problem contained in equations (1) through (3) can be specialized to a weight minimization problem by deleting $E(d,t)$ from equation (1) and adding a control effort constraint

$$E^u \geq \int_0^{t_f} E(d,t)dt = E(d) \tag{5}$$

or, alternatively the basic problem statement can be specialized to a minimum control effort problem by deleting $W(d)$ from equation (1) and adding a weight constraint

$$W^u \geq W(d) \tag{6}$$

In this paper the approximation concepts approach (e.g., see Refs. 10 and 11) is extended to control augmented structural synthesis problems with time parametric constraints and nonlinear on/off controllers. This is accomplished by replacing the time parametric constraints with a finite number of regular constraints corresponding to response peaks and then using hybrid approximations (see Ref. 12) to replace these implicit constraint functions with explicit

approximations in terms of the design variables. Move limits are used on the design variables to protect the quality of each approximate problem. The approximate form of the weight minimization problem becomes

$$\min \tilde{W}(d) \tag{7}$$

subject to

$$\tilde{g}_m(d) \geq 0 \tag{8}$$

$$E^u \geq \tilde{E}(d) \tag{9}$$

and

$$d^l \leq d \leq d^u \tag{10}$$

and the approximate form of the control effort minimization problem becomes

$$\min \tilde{E}(d) \tag{11}$$

subject to

$$\tilde{g}_m(d) \geq 0 \tag{12}$$

$$W^u \geq \tilde{W}(d) \tag{13}$$

and

$$d^l \leq d \leq d^u \tag{14}$$

where $\tilde{g}_m(d)$ and $\tilde{E}(d)$ denote explicit hybrid approximations.

Solution of either the weight minimization problem specified in equations (1) through (3) and (5) or the control effort minimization

specified in equation (1) through (3) and (6) proceeds as a sequence of solutions of the approximate problem given by either equations (7) through (10) or equations (11) through (14). The steps necessary for the solution of the approximate problem are: 1) analysis of the structure at the current design; 2) evaluation of the behavior constraints; 3) deletion of the non-critical constraints; 4) computation of sensitivities of the retained constraints with respect to all design variables; 5) solution of the approximate problem using a mathematical programming method, such as CONMIN [13]; and 6) recovery of element physical dimensions from the optimization variables to yield a new current design.

There are a number of advantages to using this type of solution method. First, the method replaces an implicit problem with a sequence of explicit problems. Second, the size of each approximate optimization problem is relatively small due to the use of design element linking and temporary constraint deletion. Third, convergence of the method is rapid provided a thoughtful choice of design variables is made so that the approximations are of high quality.

Analysis Methodology

Using a finite element representation of a control-augmented structure, the system equations of motion can be written as

$$M_{ji}\ddot{X}_i + K_{ji}X_i = P_j + B_{jn}u_n \tag{15}$$

where M_{ji} is the system mass matrix, K_{ji} is the system stiffness matrix, P_j is the vector of nodal external excitation forces, B_{jn} is a matrix of zeroes and ones placing the control actuators at nodal degrees-of-freedom, u_n is the vector of actuator force outputs, and X_i is the vector of nodal displacements and rotations. In the dynamic case, the external forces, the actuator force outputs, and the nodal displacements and rotations are time dependent. In the static case the equations of motion reduce to

$$K_{ji}X_i^s = P_j^s \tag{16}$$

where the s superscript is used to indicate static displacements and loads.

Vectors of observed displacements and velocities, Y_n and $\dot{Y}_n$, respectively, are available from the control system sensors and are given by

$$Y_n = C_{ni}X_i \tag{17}$$

and

$$\dot{Y}_n = C_{ni}\dot{X}_i \tag{18}$$

where C_{ni} is a matrix of zeroes and ones locating the control sensors at nodal degrees-of-freedom.

The normal mode method of analysis [14] is used to obtain the time dependent displacements, velocities, and accelerations which are solutions to equation (15). The normal mode method consists of two basic steps: 1) uncoupling of the equations of motion through usage of the system eigenvalues and eigenvectors; and 2) time stepping for

the dynamic modal response followed by transformation back to the physical degrees-of-freedom.

The normal mode method of analysis is based on the use of a modal transformation

$$X_i = \phi_{ik} q_k \tag{19}$$

where the modal matrix, ϕ_{ik}, is a matrix of spatial patterns and the modal response, q_k , is a vector of time dependent normal coordinates.

Introduction of the modal transformation given by equation (19) into (15) and pre-multiplication by the transpose of the modal matrix yields

$$\ddot{q}_k + 2\zeta_k \omega_k \dot{q}_k + \omega_k^2 q_k = Q_k + Z_k \tag{20}$$

where the vector of modal excitation forces, Q_k, is given by

$$Q_k = \phi_{jk} P_j \tag{21}$$

the vector of modal control forces, Z_k, is given by

$$Z_k = \phi_{jk} B_{js} u_s \tag{22}$$

and ζ_k and ω_k are the kth modal damping ratio and kth natural frequency, respectively.

Solution for the modal response from equation (20) proceeds very rapidly with the use of the Wilson-θ time stepping method [15]. The Wilson-θ method is an explicit time integration method which is unconditionally stable for any time step size provided that the θ parameter is greater than 1.37. Physical degree-of-freedom responses

can be obtained at each time step using the modal transformation in equation (19).

Behavior constraints are readily evaluated from the physical degree-of-freedom responses and non-critical constraints can now be deleted from further consideration during the current approximate problem solution.

Calculation of Sensitivities

Behavior sensitivities for the static displacements are calculated using the partial inverse form of the pseudo-load method [16], eigenvalue sensitivities are calculated using the method outlined by Fox and Kapoor [17], and Nelson's method [18] is used to determine the eigenvector sensitivities.

Time parametric transient displacement and acceleration sensitivities can be obtained by differentiating the modal transformation in equation (19) to give

$$\frac{\partial X_i}{\partial d_r} = \frac{\partial \phi_{ik}}{\partial d_r} q_k + \phi_{ik} \frac{\partial q_k}{\partial d_r} \tag{23}$$

and

$$\frac{\partial \ddot{X}_i}{\partial d_r} = \frac{\partial \phi_{ik}}{\partial d_r} \ddot{q}_k + \phi_{ik} \frac{\partial \ddot{q}_k}{\partial d_r} \tag{24}$$

The difficult terms to obtain, $\partial q_k / \partial d_r$ and $\partial \ddot{q}_k / \partial d_r$, can be computed in an efficient manner by writing the modal equations of motion in first order form as

$$\begin{bmatrix}\dot{\eta}_1\\ \dot{\eta}_2\end{bmatrix}=\begin{bmatrix}0 & 1\\ -\alpha_1 & -\alpha_2\end{bmatrix}\begin{bmatrix}\eta_1\\ \eta_2\end{bmatrix}+\begin{bmatrix}0\\ 1\end{bmatrix}Q+\begin{bmatrix}0\\ 1\end{bmatrix}Z \tag{25}$$

where it is understood that $\eta_1 = q$, $\eta_2 = \dot{q}$, and the essential parameters are defined as $\alpha_1 = \omega^2$ and $\alpha_2 = 2\zeta\omega$. Now rewrite equation (25) in compact form

$$\dot{\eta} = \overline{A}\eta + bQ + bZ \tag{26}$$

and apply the Wilkie-Perkins [19] essential parameter method.

The Wilkie-Perkins essential parameter method takes advantage of the special form of the $\overline{A}$ matrix to reduce the amount of time stepping needed in calculating the time parametric transient response sensitivities. In this manner, the sensitivities are obtained by: (1) time stepping K sets of equation (27)

$$\frac{\hat{c}\dot{\eta}}{\hat{c}\alpha_1}\Big|_{t+\Delta t} = [\overline{A}]\frac{\hat{c}\eta}{\hat{c}\alpha_1}\Big|_t + \left[\frac{\hat{c}\overline{A}}{\hat{c}\alpha_1}\right]\eta\Big|_t \tag{27}$$

(2) utilizing the relations

$$\frac{\hat{c}\eta_1}{\hat{c}\alpha_2} = \frac{\hat{c}\eta_2}{\hat{c}\alpha_1} \tag{28}$$

and

$$\frac{\hat{c}\eta_2}{\hat{c}\alpha_2} = -\eta_1 - \alpha_1\frac{\hat{c}\eta_1}{\hat{c}\alpha_1} - \alpha_2\frac{\hat{c}\eta_2}{\hat{c}\alpha_1} \tag{29}$$

and (3) transforming essential parameter sensitivities to design variable sensitivites by

$$\frac{\hat{c}}{\hat{c}d_r} = \frac{\hat{c}}{\hat{c}\alpha_1}\frac{\hat{c}\alpha_1}{\hat{c}d_r} + \frac{\hat{c}}{\hat{c}\alpha_2}\frac{\hat{c}\alpha_2}{\hat{c}d_r} \tag{30}$$

The computational effort required will now be that needed for time stepping solutions of K sets of equation (25) for the system response and K sets of equation (27) for the modal response sensitivities where K is the number of retained modes.

It should be noted that this method of obtaining sensitivities can only be used for the passive structural design variables because the essential parameters, α_1 and α_2, are independent of the active control design variables. For the active control variables, the sensitivity equations are obtained by differentiating equation (26) with respect to the control design variables to yield

$$\frac{\partial \dot{\eta}}{\partial d_r}\Big|_{t+\Delta t} = [\overline{A}]\frac{\partial \eta}{\partial d_r}\Big|_t + b\frac{\partial Z}{\partial d_r}\Big|_t \tag{31}$$

Active control sensitivities are obtained using the finite difference method on equation (31) because of the complex form of the control laws.

The Wilkie-Perkins essential parameter method is well suited for further efficiency improvements if parallel processing facilities are available since the sensitivity of each mode is calculated independently of all other modes.

Once the sensitivities have been obtained, construction of the current approximate problem is straightforward. Each approximate problem is solved using CONMIN [13] and then the cross sectional dimensions corresponding to the final values of the direct section properties are obtained using a linearized recovery scheme [11].

Numerical Examples

In this section numerical results for some example problems are presented. All of the examples presented here are minimum weight design problems. The problems were solved using a research-level computer code written on an IBM AT personal computer and modified to run on an FPS-164 computer.

Planar Grillage Structure - Case 1

The twenty-one degree-of-freedom planar grillage structure shown in Figure 3 will be used here for examples where weight minimization is selected as the design objective. The structural material is taken to be aluminum (see Table 1 for material properties) and the grillage is subjected to the transient force-time history shown in Figure 3. The load is applied at node 8, slightly off the centerline of the structure, so that both symmetric and non-symmetric modes are excited. Behavior constraints are placed on the vertical dynamic displacement at nodes 2, 4, 5, 6, and 7 (see Table 1 for specific limiting values). The dynamic analyses were carried out using ten retained modes (frequency content up to 100 Hz), a final integration time of 1.0 second, a time step size of 0.0005 seconds, and 2% modal damping (i.e., $\zeta = 0.02$). All relevant input information is shown in Table 1.

The minimum weight design of this structure is sought for the uncontrolled case, for the controlled case using one colocated sensor/actuator at node 6, and for the controlled case using two colocated sensor/actuators located at nodes 5 and 7. All controlled

cases were run using both the Type I actuators and the Type II actuators giving a total of five design subcases.

Iteration histories for the uncontrolled design, single Type I actuator controlled design, and two Type I actuator controlled design are shown in Figure 4. (Open symbols denote feasible designs while solid symbols denote infeasible designs for all iteration histories in Figures 4-7.) Table 2 contains the optimum design and the critical constraints for all of these subcases.

A minimum mass of 538 kilograms was obtained for the optimum design of the uncontrolled structure. Because the structure acts primarily like a cantilever, design elements 3, 4, and 5 reach their minimum gage thicknesses at the optimum design and the dynamic displacements at nodes 6 and 7 reach their upper limit. The optimum design tapers down from root to tip as expected.

An optimum design of 377 kilograms, 29.9% lighter than the uncontrolled design, can be obtained with the introduction of a single Type I actuator at node 6. The dynamic displacement constraint for node 7 is critical at the optimum design indicating that the control system is effective at controlling bending response but is unable to control torsional effects due to its location on the center line of the structure.

In order to try and control bending behavior and torsional behavior simultaneously, two Type I actuators were placed on the structure; one at node 5 and one at node 7. The resulting optimum design has a mass of 375 kilograms, not significantly lower than that obtained with one

actuator, but the design and critical constraints are completely different. The critical constraints at the optimum design for the two actuator subcase are the dynamic displacement constraints at nodes 5, 6, and 7 and the control system effort constraint ($E = 55$ N^2-sec). These critical constraints suggest that torsional effects have been controlled, but the control system effort constraint is hit before bending effects can be controlled in a more efficient manner than was done using a single actuator at node 6.

Iteration histories for the uncontrolled design, single Type II actuator controlled design, and two Type II actuator controlled design are shown in Figure 5. Table 3 contains the optimum design and the critical constraints for all of these subcases.

The optimum design for the single Type II actuator controlled design is 346 kilograms, 30.2% lighter than the uncontrolled optimum design. The critical constraints, namely the dynamic displacement at node 7, the actuator force upper bound, and the lower bound beam thickness dimensions for design elements 3, 4, and 5, suggest that bending effects are being controlled. However, torsional effects cannot be controlled due to the location of the actuator on the center line of the structure.

Simultaneous bending-torsion control was attempted using two Type II actuators, one at node 5 and one at 7. The two Type II actuator subcase yields a minimum mass of 259 kilograms, 51.9% lighter than the uncontrolled minimum mass design. The critical constraints are the dynamic displacement at node 6, the actuator force upper bound for the

actuator at node 7, and the beam thickness lower bounds for design elements 2, 3, 4, and 5. This critical constraint combination implies that control of the torsional effects can be achieved in conjunction with control of the bending effects by using two Type II actuators. It is observed that the actuator force at node 7 reaches its upper bound, thereby reducing the torsional effects of the excitation, and letting both actuators combine to reduce the bending effects.

Planar Grillage Structure - Case 2

The minimum weight design of the planar grillage structure is sought where constraints are placed on the peak transient accelerations at nodes 2, 4, 5, 6, and 7 in addition to the constraints on peak transient displacements considered previously. Furthermore, spherical nonstructural mass design elements are used to represent the mass of sensor/actuator pairs for the controlled cases. Each nonstructural mass design element has a density of $\rho = 2770\ \mathrm{kg/m^3}$ with the initial radius set equal to a lower bound value of 0.10 meters (initial mass of 11.6 kg).

Optimum designs are sought for the uncontrolled structure, for the controlled structure using three Type I sensor/actuator pairs at nodes 2, 4, and 6, and for the controlled structure using four Type I sensor/actuator pairs located at nodes 2, 4, 5, and 7. All control configurations were also run using Type II actuators.

The optimum design for the uncontrolled transient displacement and transient acceleration constrained grillage structure is given in Table

4 while iteration histories for all Case 2 optimum design problems are shown in Figures 6 and 7. The critical constraints at the optimum design are the peak dynamic displacement constraints at nodes 5 and 7 and the peak acceleration constraints at nodes 2, 4, and 6. This combination of critical constraints suggests that the structure acts predominantly like a cantilever beam without significant torsional effects.

Optimum designs for the three and four Type I actuator controlled grillage structures are shown in Table 4 along with the uncontrolled optimum design. The addition of three Type I actuators yields an optimum design that is 14.0% lighter than the uncontrolled design. The four Type I controlled configuration has an optimum design that is 13.0% lighter than the uncontrolled structure. In both Type I controlled cases the control system acts to control dynamic displacements while the structural system reduces dynamic acceleration constraints by taking the form of a combined cantilever-torsional mass damper. It should be noted that these lighter designs were obtained despite the large mass penalty (11.6 kg) assigned to each sensor/actuator pair.

Optimum designs for the Type II controlled planar grillage structure can be found in Table 5. Three Type II actuators lead to an optimum design that is 31.1% lighter than the uncontrolled optimum design and 19.8% lighter than the optimum design found using three Type I actuators. Four Type II actuators yield an optimum design that is 30.7% lighter than the uncontrolled optimum design and 20.4% lighter

than the four Type I actuator controlled case. For both of the Type II controlled cases, the optimum design resembles a torsional mass damper and all of the actuator force levels fall between 8.27 and 6.95 Newtons.

If the mass penalty assigned to each actuator was lower, then the mass saving achieved by adding the fourth actuator might exceed the mass increase associated with adding it. Furthermore, if the loading function excited higher modes that had to be retained in the dynamic response calculations, it might be necessary to utilize additional actuators to control these extra modes.

This planar grillage structure example problem illustrates the beneficial effect that the addition of a control system can have on the resulting optimum design when forethought is given to the use and placement of the actuators. By judicious placement of the actuators, the primary modes participating in the response can be controlled with relatively low actuator output force levels, leading to lighter optimum designs in spite of the deliberately heavy weight penalty associated with each sensor/actuator pair.

Concluding Remarks

The control augmented structural synthesis approach has been successfully extended to systems involving general transient response and nonlinear on/off controllers. An important feature of this work is that limitations on dynamic response and actuator force levels are

met by treating them as direct behavior constraints, rather than by incorporating them into a system performance index. Herein the integrated structures/control system design problem was first formulated as a nonlinear mathematical programming problem involving time parametric constraints. Solutions were then obtained by solving a sequence of approximate problems. These approximate problems were constructed by first replacing the time parametric constraints with a finite number of regular constraints corresponding to response peaks and then using hybrid approximations to generate explicit representations of these constraints in terms of the independent design variables. The efficiency of the dynamic response sensitivity analysis was improved significantly by applying the Wilkie-Perkins essential parameter method. The optimization procedure also incorporates design variable linking and constraint deletion features. Numerical results for an example problem, which exhibits characteristics representative of more complex systems, indicates that substantial improvement can be achieved through integrated design optimization of structures and controls.

REFERENCES

1 Horner, G. C ., "Optimum Actuator Placement, Gain, and Number for a Two-Dimensional Grillage", AIAA Paper No. 83-0854, 1983.

2 Horner, G. C. and Walz, J. E., "A Design Technique for Determining Actuator Gains in Spacecraft Vibration Control", AIAA Paper No. 85-0628, 1985.

3 Oz, H. and Meirovitch, L., "Optimal Modal Space Control of Flexible Gyroscopic Systems", Journal of Guidance and Control, and Dynamics, Vol. 3, May-June 1980, pp. 218-226.

4 Haftka, R. T., Martinovic, Z. N., and Hallauer, W. L., "Enhanced Vibration Contollability by Minor Structural Modifications", AIAA Paper No. 84-1036, 1984.

5 Venkayya, V. B. and Tischler, V. A., "Frequency Control and the Effect on the Dynamic Response of Flexible Structures", AIAA Paper No. 84-1044, 1984.

6 Khot, N. S., Eastep, F. E. and Venkayya, V. B., "Optimal Simultaneous Structural and Control Design of Maneuvering Flexible

Spacecraft", Journal of Guidance, Control, and Dynamics, Vol. 8, No. 1, Jan.-Feb. 1985, pp. 86-93.

7 Messac, A. and Turner, J., "Dual Structural-Control Optimization of Large Space Structures", presented at the NASA Symposium on Recent Experiences in Multidisciplinary Analysis and Optimization, April 1984.

8 Junkins, J. L., Bodden, D. S., and Turner, J. D., "A Unified Approach to Structure and Control System Design Iterations", presented at the Fourth International Conference on Applied Numerical Modeling, Tainan, Taiwan, December 1984.

9 Bodden, D. S. and Junkins, J. L., "Eigenvalue Optimization Algorithms for Structure/Controller Design Iterations", Journal of Guidance, Control, and Dynamics, Vol. 8, No. 6, Nov.-Dec. 1985, pp. 697-706.

10 Lust, R. V. and Schmit, L. A., "Control Augmented Structural Synthesis", paper presented at the 26th AIAA/ASME/ASCE/AHS Structures, Structural Dynamics, and Materials Conference, San Antonio, Texas, May 17-19, 1986.

11 Lust, R. V. and Schmit, L. A., "Alternative Approximation Concepts for Space Frame Synthesis", NASA CR 172526, March 1985.

12 Starnes, J. H., Jr. and Haftka, R. T., "Preliminary Design of Composite Wings for Buckling, Stress, and Displacement Constraints", Journal of Aircraft, Vol. 16, August 1979, pp. 564-570.

13 Vanderplaats, G. N., "CONMIN - A Fortran Program for Constrained Function Minimization", NASA TM X-62,282, August 1973.

14 Meirovitch, L., "Analytical Methods in Vibrations", MacMillan, New York, 1967.

15 Bathe, K., and Wilson, E. L., "Numerical Methods in Finite Element Analysis", Prentice Hall, Inc., Englewood Cliffs, New Jersey, 1976.

16 Schmit, L. A. and Miura, H., "Approximation Concepts for Efficient Structural Synthesis", NASA CR 2552, March 1976.

17 Fox, R. L. and Kapoor, M. P., "Rate of Change of Eigenvalues and Eigenvectors", AIAA Journal, Vol. 6, No. 12, 1968, pp. 2426-2429.

18 Nelson, R. B., "Simplified Calculation of Eigenvector Derivatives", AIAA Journal, Vol. 14, No. 9, 1976, pp. 1201-1205.

19 Wilkie, D. F. and Perkins, W. R., "Essential Parameters in Sensitivity Analysis", Automatica, Vol. 5, 1969, pp. 191-197.

Appendix A

CONTROL LAW DESCRIPTION

The first type of actuator, referred to hereafter as a Type I actuator, utilizes both displacement and velocity measurements and produces output forces according to the relations

$$u_n = \begin{cases} 0 \text{ if } |Y_n| \le \delta_n \\ -\bar{u}_n \text{ if } |Y_n| \ge \delta_n \text{ and } Y_n \ge 0 \text{ and } \dot{Y}_n \ge 0 \\ -\bar{u}_n \text{ if } |Y_n| \ge \delta_n \text{ and } Y_n \ge 0 \ge \dot{Y}_n \text{ and } |\dot{Y}_n| \le \varepsilon_n \\ +\bar{u}_n \text{ if } |Y_n| \ge \delta_n \text{ and } Y_n \le 0 \text{ and } \dot{Y}_n \le 0 \\ +\bar{u}_n \text{ if } |Y_n| \ge \delta_n \text{ and } Y_n \le 0 \le \dot{Y}_n \text{ and } |\dot{Y}_n| \le \varepsilon_n \\ 0 \text{ otherwise} \end{cases} \tag{A.1}$$

where ε_n is the velocity threshold, δ_n is the magnitude of the deadband region, and u_n is the magnitude of the output force. Figure 8 graphically shows the control law described in equation (A.1) for a typical observed time history with $\delta = 0.2$ and $\varepsilon = 5.0$.

The presence of the deadband region and velocity threshold parameters indicate that a small amount of vibration about the zero displacement point is allowed, but any vibration past this region activates the control system.

The second type of actuator, hereafter referred to as a Type II actuator, utilizes only velocity measurements and produces output forces according to the relations

$$u_n = \begin{cases} 0 \text{ if } |\dot{Y}_n| \le \varepsilon_n \\ -\bar{u}_n \text{ if } |\dot{Y}_n| \ge \varepsilon_n \text{ and } \dot{Y}_n \ge 0 \\ +\bar{u}_n \text{ if } |\dot{Y}_n| \ge \varepsilon_n \text{ and } \dot{Y}_n \le 0 \\ 0 \text{ otherwise} \end{cases} \tag{A.2}$$

where again a small amount of vibration is tolerable. Figure 9 graphically depicts the control law described by equation (A.2) for the same observed time history with $\varepsilon = 5.0$.

For the Type I actuator, the velocity threshold, ε_n , is preassigned and the design variables are the size of the deadband region, δ_n , and the output force, $\bar{u}_n$. For the Type II actuator, the velocity threshold, ε_n, and the output force, $\bar{u}_n$, are selected as design variables.

The locations of both the sensors and the actuators are fixed during the design process. Finally, two options for control system effort are available. The first is the quadratic form

$$E = \int_0^{t_f} u_n^2(d,t)dt \tag{A.3}$$

where t_f is the final integration time in the analysis. The second option is the linear form

$$E = \int_0^{t_f} |u_n(d,t)|\, dt \tag{A.4}$$

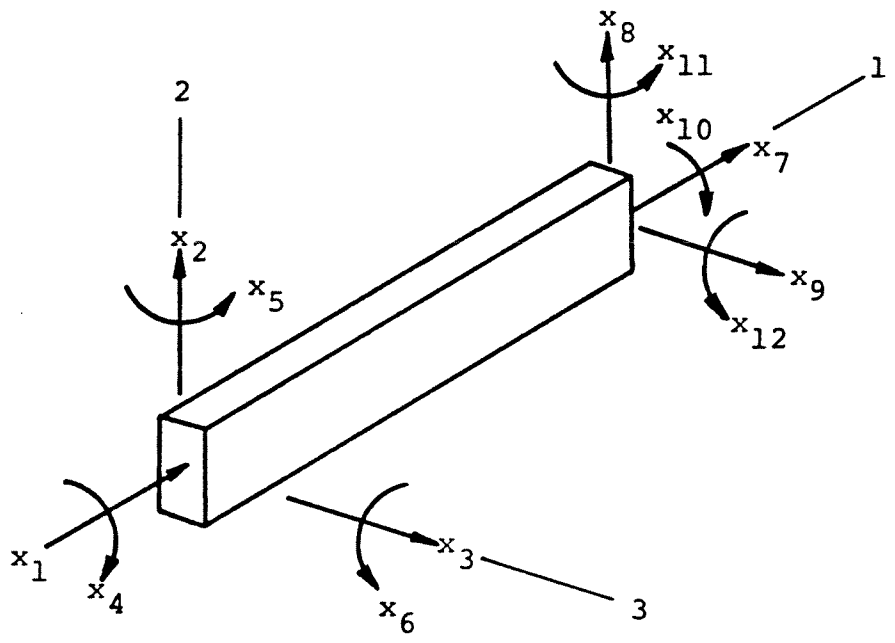

Figure 1: Twelve Degree-of-Freedom Box Beam Finite Element

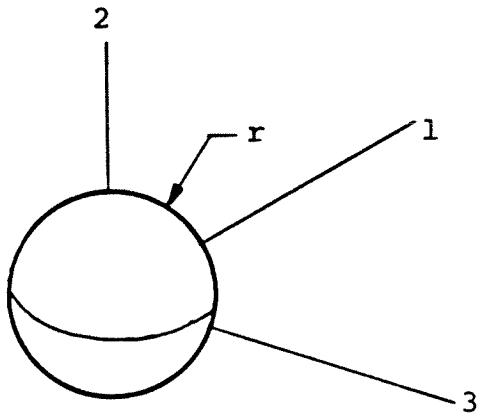

Figure 2: Spherical Nonstructural Mass Design Element

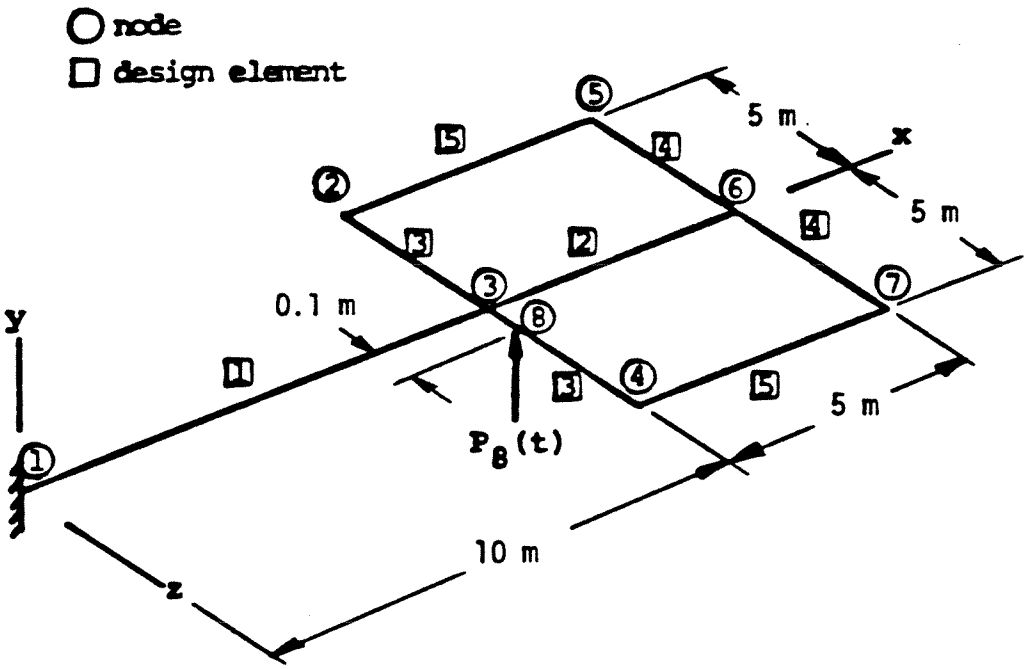

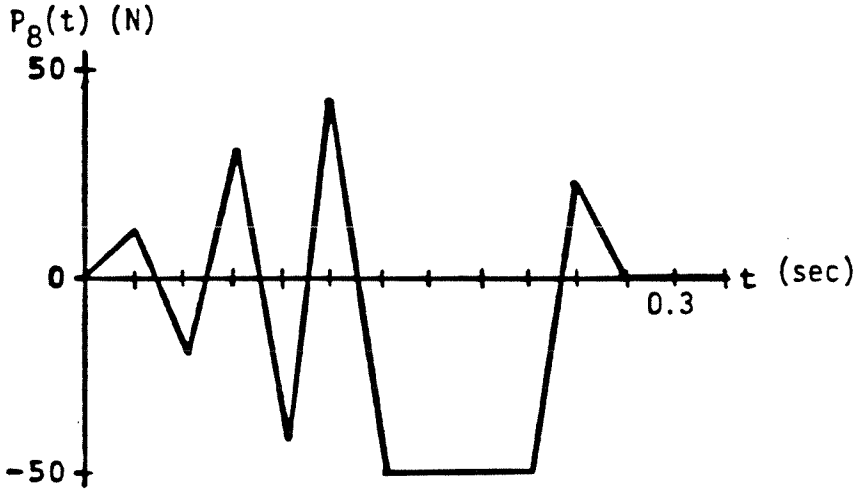

Figure 3: Twenty-One Degree-of-Freedom Planar Grillage Example

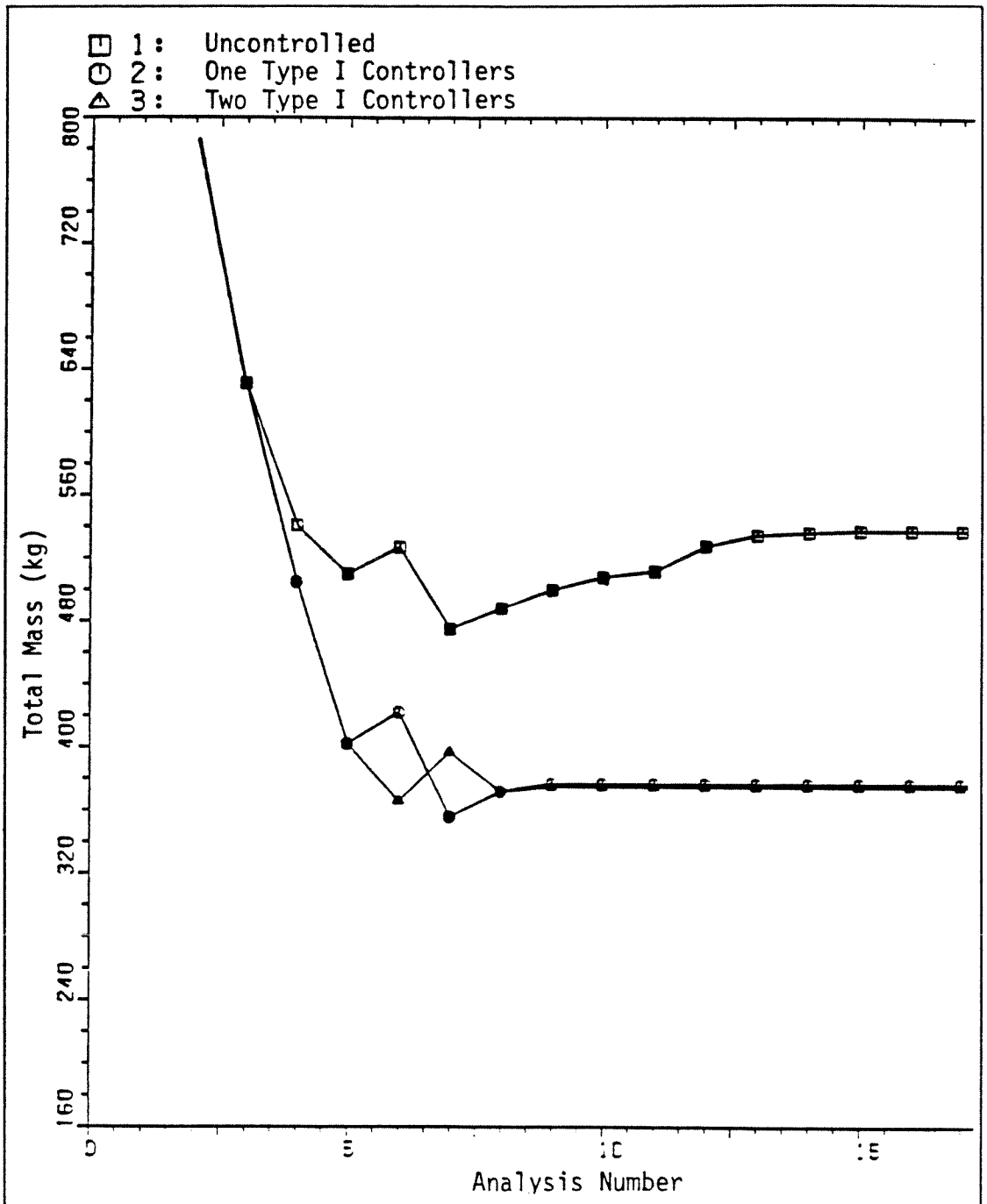

Figure 4: Iteration Histories for the Planar Grillage (Case 1 - Type I)

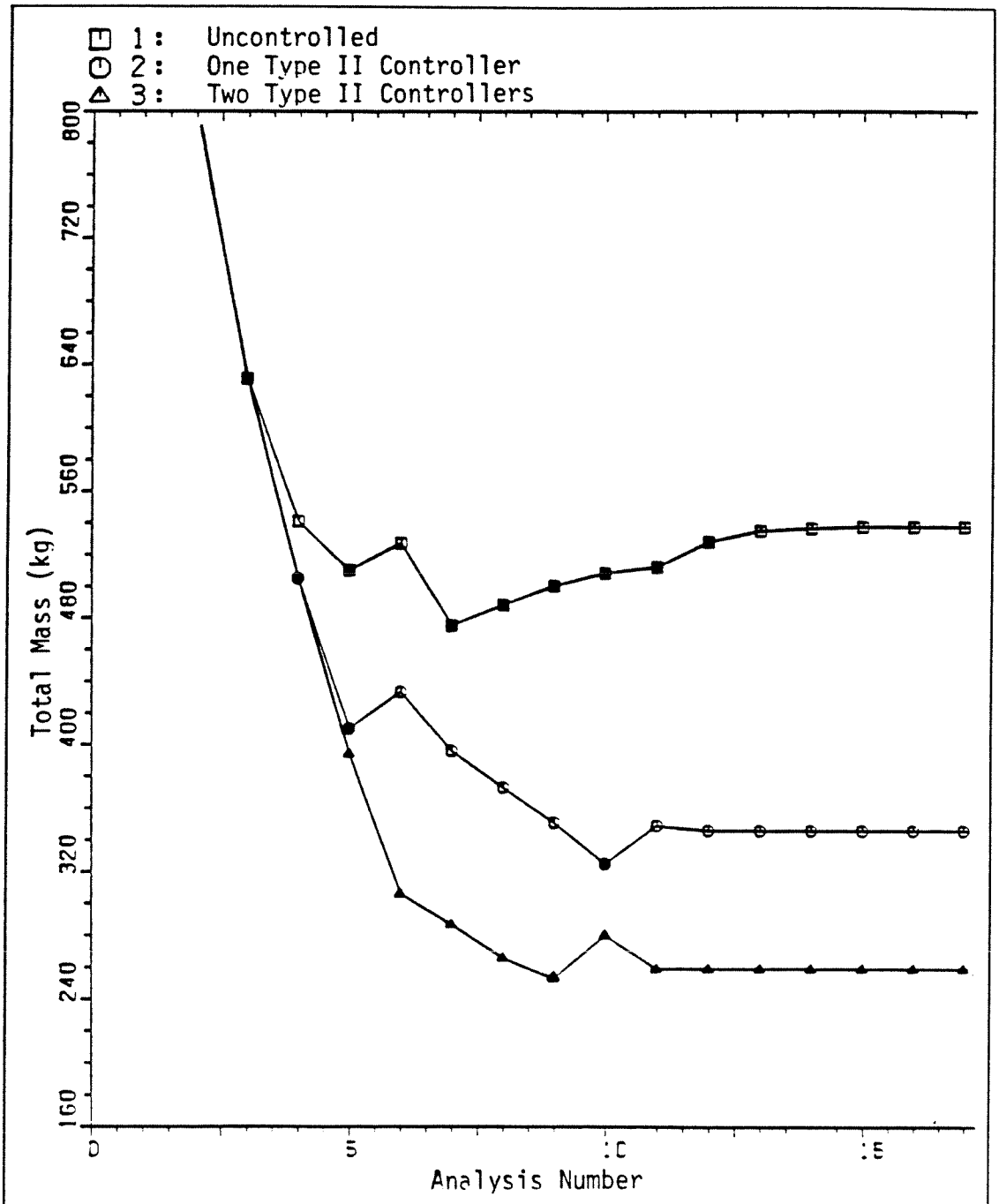

Figure 5: Iteration Histories for the Planar Grillage (Case 1 - Type II)

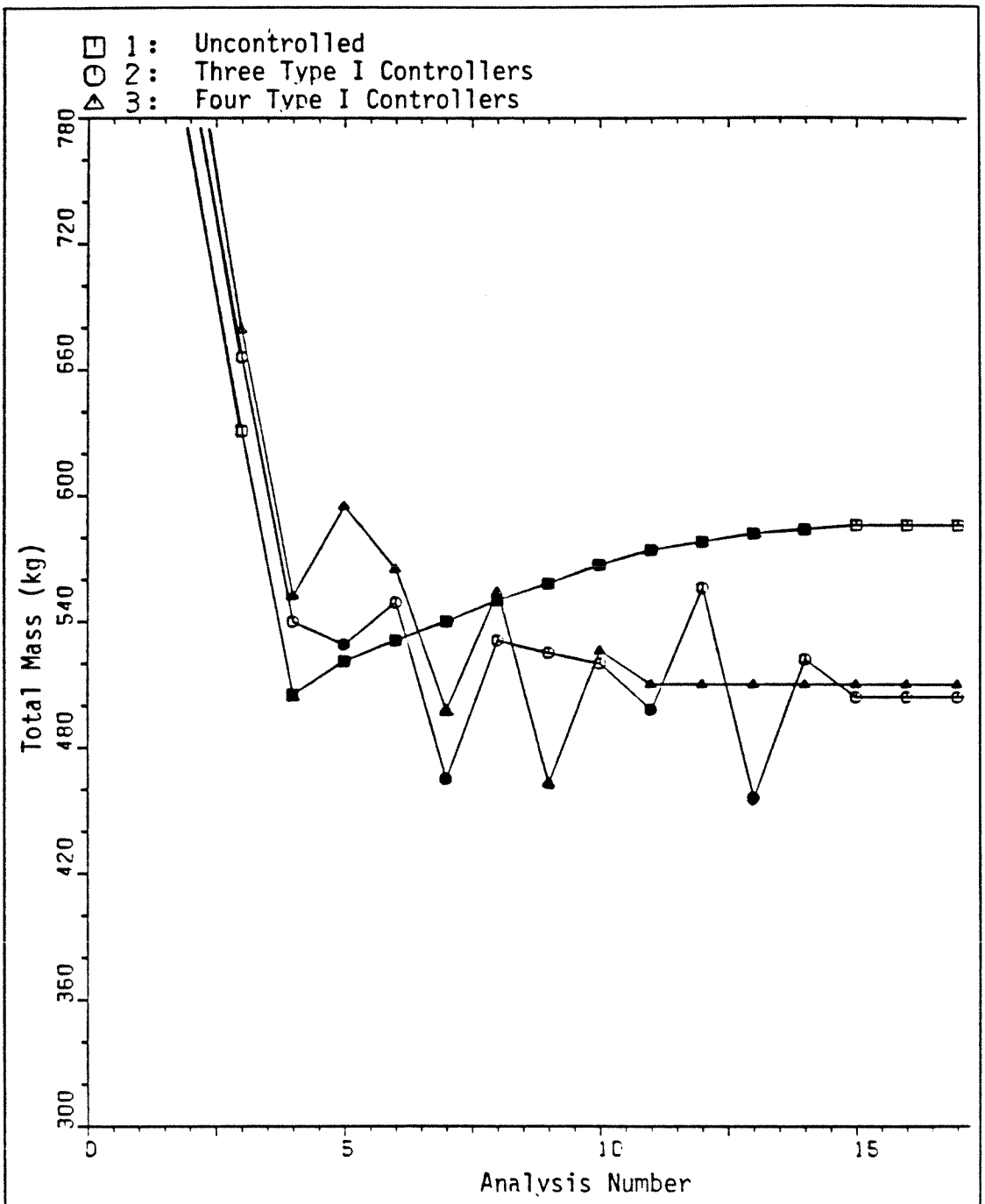

Figure 6: Iteration Histories for the Planar Grillage (Case 2 - Type I)

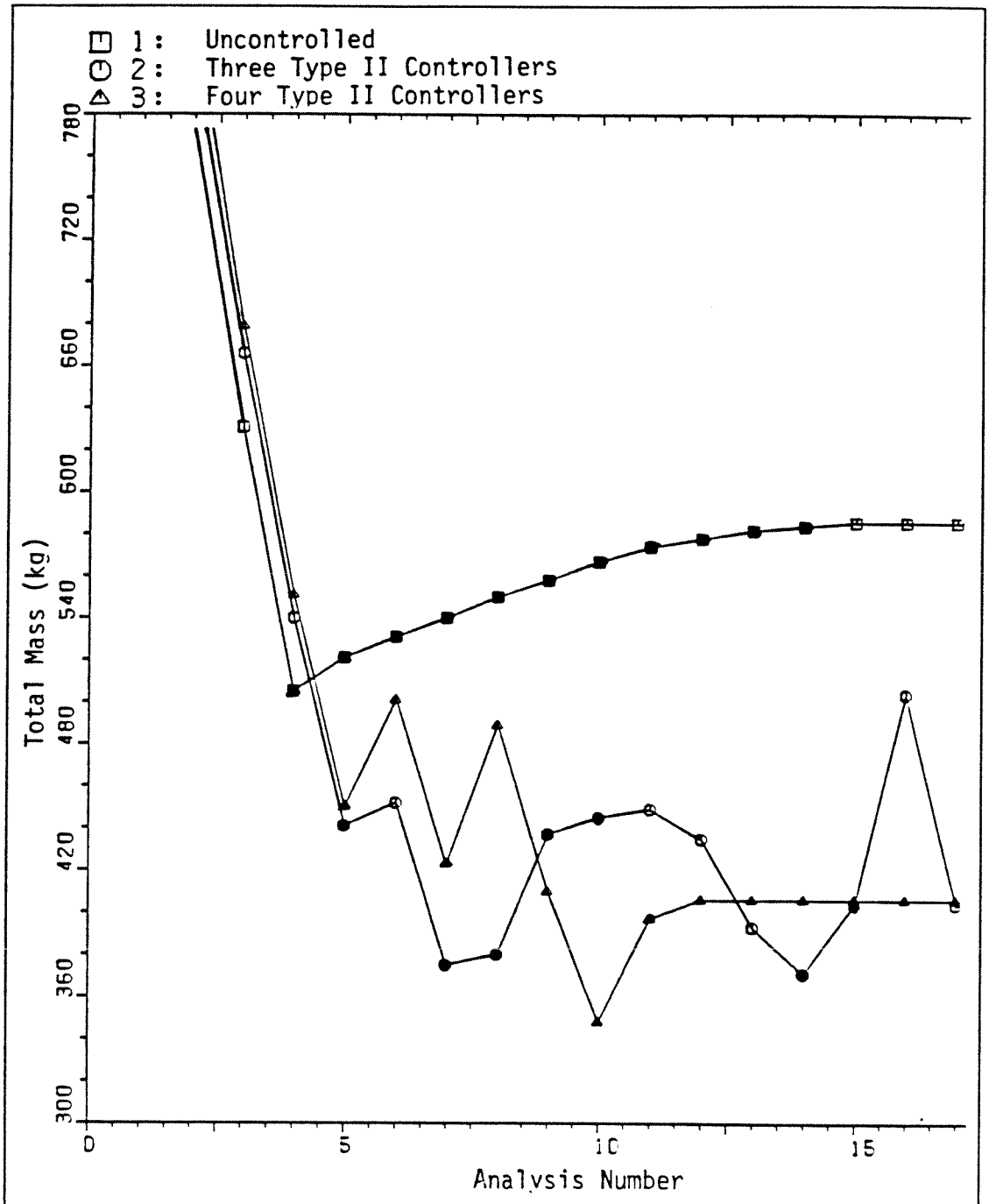

Figure 7: Iteration Histories for the Planar Grillage (Case 2 - Type II)

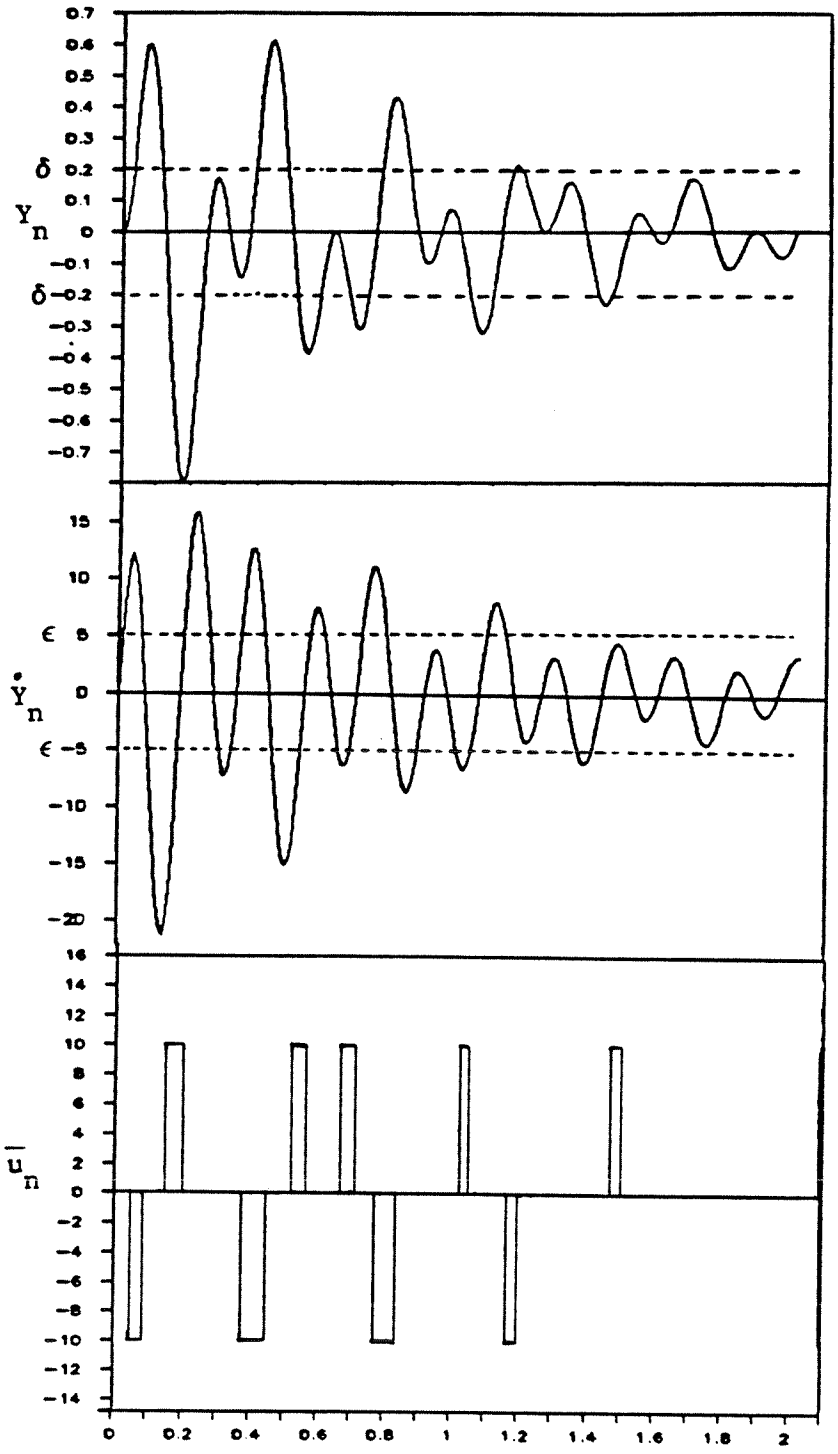

Figure 8: Actuator Outputs for Displacement Actuator (Type I)

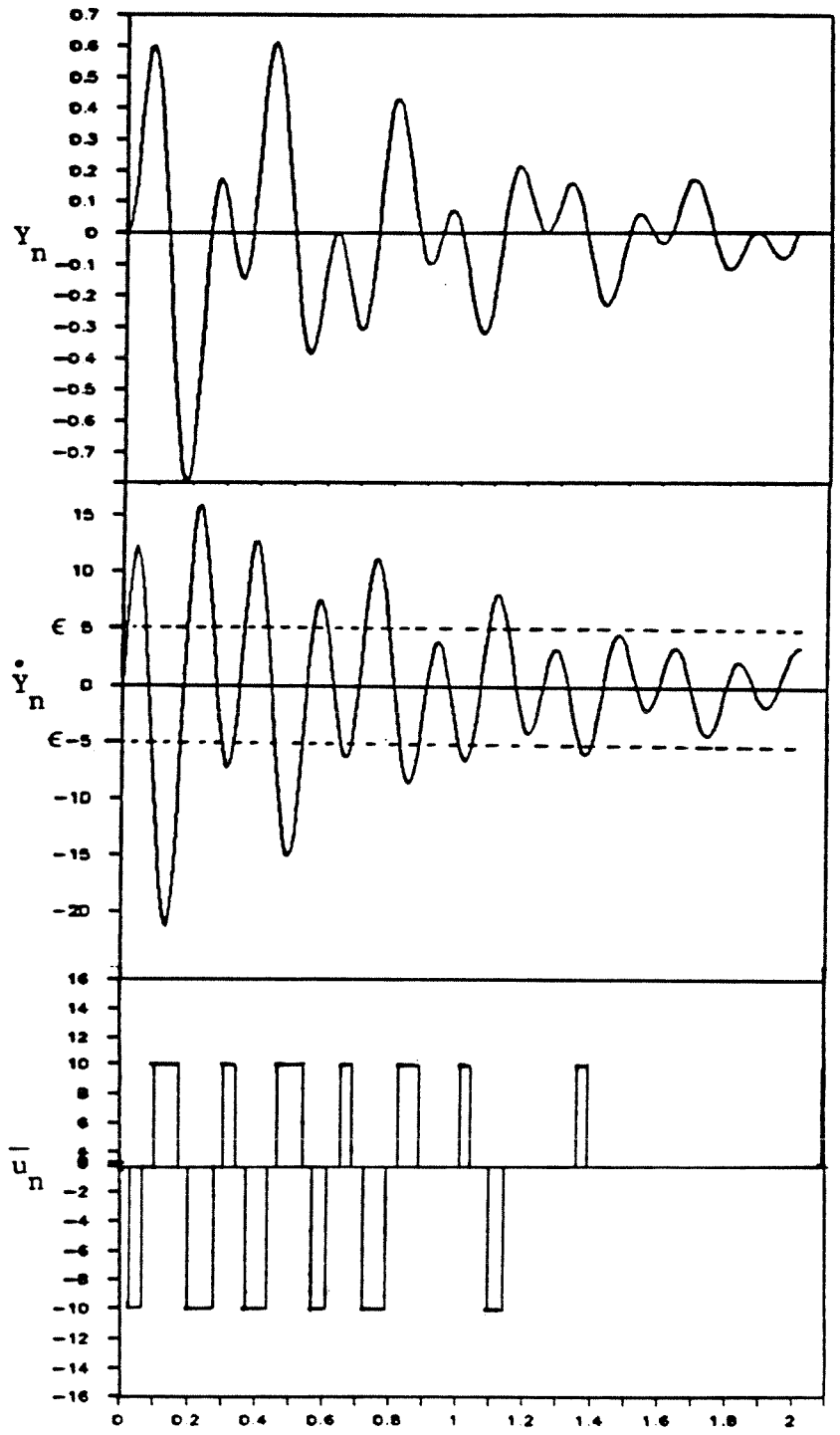

Figure 9: Actuator Outputs for Velocity Actuator (Type II)

TABLE 1

Planar Grillage Example Input Data

Material Properties:	$E = 7.3 \times 10^{10}$ N/m^2 $\rho = 2770$ kg/m^3 $\nu = 0.325$
Loading:	(See Figure 3)
Dynamic Constraints:	$\lvert X_{y2}, X_{y4} \rvert < 7.5 \times 10^{-4}$ m $\lvert X_{y5}, X_{y6} \rvert < 9.0 \times 10^{-4}$ m $\lvert X_{y7} \rvert < 9.0 \times 10^{-4}$ m $\lvert \ddot{X}_{y2}, \ddot{X}_{y4} \rvert < 7.5$ m/sec^2 $\lvert \ddot{X}_{y5}, \ddot{X}_{y6} \rvert < 9.0$ m/sec^2 $\lvert \ddot{X}_{y7} \rvert < 9.0$ m/sec^2
Control Constraints:	$E < 55.0\ N^2 - \text{sec}$
CSD Variable Linking:	$B,H = 0.5$ m fixed, $t_2 = t_3$ $\varepsilon = 0.01$m/sec fixed (Type I only)

Side Constraints

Variable	Units	Lower Bound	Initial Design	Upper Bound
B	m	0.10	0.50	2.00
H	m	0.10	0.50	2.00
t_2	m	0.001	0.005	0.02
t_3	m	0.001	0.005	0.02
r	m	0.1	0.1	2.0
δ	m	0.0001	0.0002	0.0008
ε	m/sec	0.001	0.005	1.00
$\bar{u}$	N	0.1	5.0	10.0

TABLE 2

Planar Grillage Optimal Designs - Case 1

(Type I Actuators)

Design Variables	Units	Uncontrolled	1 Type I Actuator	2 Type I Actuators
Beam 1 t	m	0.0060	0.0018	0.0019
Beam 2 t	m	0.0015	0.0015	0.0019
Beam 3 t	m	0.0010	0.0011	0.0011
Beam 4 t	m	0.0010	0.0020	0.0017
Beam 5 t	m	0.0010	0.0012	0.0012
Node 5 δ	m	------	------	0.0002
Node 5 $\bar{u}$	N	------	------	6.77
Node 6 δ	m	------	0.0001	-----
Node 6 $\bar{u}$	N	------	9.25	-----
Node 7 δ	m	------	------	0.0002
Node 7 $\bar{u}$	N	------	------	6.40
Total Mass	kg	538	377	375
Critical Constraints		t_3^-, t_4^-, t_5^- X_{y6}, X_{y7}	X_{y7}	E, X_{y5}, X_{y6} X_{y7}

$^+$Design variable at upper bound

$^-$Design variable at lower bound

Subscripts on r and u indicate nodal locations

TABLE 3

Planar Grillage Optimal Designs - Case 1

(Type II Actuators)

Design Variables	Units	Uncontrolled	1 Type II Actuator	2 Type II Actuators
Beam 1 t	m	0.0060	0.0025	0.0012
Beam 2 t	m	0.0015	0.0014	0.0010
Beam 3 t	m	0.0010	0.0010	0.0010
Beam 4 t	m	0.0010	0.0011	0.0010
Beam 5 t	m	0.0010	0.0010	0.0010
Node 5 ε	m/s	------	------	0.0016
Node 5 $\bar{u}$	N	------	------	7.79
Node 6 ε	m/s	------	0.0024	-----
Node 6 $\bar{u}$	N	------	10.00	-----
Node 7 ε	m/s	------	------	0.0024
Node 7 $\bar{u}$	N	------	------	10.00
Total Mass	kg	538	346	259
Critical Constraints		t_3^-, t_4^-, t_5^- X_{y6}, X_{y7}	t_3^-, t_5^-, u_6^+ X_{y7}	t_2^-, t_3^-, t_4^- u_6^+, X_{y6}

$^+$Design variable at upper bound

$^-$Design variable at lower bound

Subscripts on r and u indicate nodal locations

TABLE 4

Antenna Structure Optimal Designs - Case 2

(Type I Actuators)

Design Variables	Units	Uncontrolled	3 Type I Actuators	4 Type I Actuators
Beam 1 t	m	0.0046	0.0011	0.0011
Beam 2 t	m	0.0016	0.0010	0.0011
Beam 3 t	m	0.0020	0.0024	0.0020
Beam 4 t	m	0.0014	0.0020	0.0021
Beam 5 t	m	0.0018	0.0019	0.0021
Node 2 r	m	------	0.121	0.122
Node 4 r	m	------	0.122	0.124
Node 5 r	m	------	------	0.102
Node 6 r	m	------	0.131	------
Node 7 r	m	------	------	0.103
Node 2 δ	m	------	0.0002	0.0003
Node 2 $\bar{u}$	N	------	3.96	3.49
Node 4 δ	m	------	0.0002	0.0002
Node 4 $\bar{u}$	N	------	4.26	2.21
Node 5 δ	m	------	------	0.0002
Node 5 $\bar{u}$	N	------	------	7.72
Node 6 δ	m	------	0.0001	-----
Node 6 $\bar{u}$	N	------	7.21	-----
Node 7 δ	m	------	------	0.0002
Node 7 $\bar{u}$	N	------	------	5.32
Structural Mass	kg	586	437	441
Total Mass	kg	586	504	510
Critical Constraints		$X_{y5}, X_{y7}, \ddot{X}_{y2}$ $\ddot{X}_{y4}, \ddot{X}_{y6}$	$\ddot{X}_{y2}, \ddot{X}_{y4}, \ddot{X}_{y6}$	$\bar{r}_5, \bar{r}_7, \ddot{X}_{y2}$ $\ddot{X}_{y4}, \ddot{X}_{y6}$

$^{+}$Design variable at upper bound

$^{-}$Design variable at lower bound

Subscripts on r and u indicate nodal locations

TABLE 5

Antenna Structure Optimal Designs - Case 2

(Type II Actuators)

Design Variables	Units	Uncontrolled	3 Type II Actuators	4 Type II Actuators
Beam 1 t	m	0.0046	0.0011	0.0012
Beam 2 t	m	0.0016	0.0011	0.0014
Beam 3 t	m	0.0020	0.0010	0.0011
Beam 4 t	m	0.0014	0.0011	0.0012
Beam 5 t	m	0.0018	0.0024	0.0016
Node 2 r	m	------	0.130	0.131
Node 4 r	m	------	0.129	0.124
Node 5 r	m	------	------	0.105
Node 6 r	m	------	0.107	------
Node 7 r	m	------	------	0.102
Node 2 ε	m/s	------	0.0034	0.0046
Node 2 $\bar{u}$	N	------	7.29	7.31
Node 4 ε	m/s	------	0.0042	0.0032
Node 4 $\bar{u}$	N	------	7.04	7.41
Node 5 ε	m/s	------	------	0.0024
Node 5 $\bar{u}$	N	------	------	7.28
Node 6 ε	m/s	------	0.0032	-----
Node 6 $\bar{u}$	N	------	8.27	-----
Node 7 ε	m/s	------	------	0.0023
Node 7 $\bar{u}$	N	------	------	6.95
Structural Mass	kg	586	339	332
Total Mass	kg	586	404	406
Critical Constraints		$X_{y5}, X_{y7}, \ddot{X}_{y2}$ $\ddot{X}_{y4}, \ddot{X}_{y6}$	$t_3^-, X_{y7}, \ddot{X}_{y5}$	$r_7^-, \ddot{X}_{y4}$

$^+$Design variable at upper bound

$^-$Design variable at lower bound

Subscripts on r and u indicate nodal locations